ACS APPLIED MATERIALS & INTERFACES

Research Article

www.acsami.org

Enhanced Performance of Nanocrystalline ZnO DNA Biosensor via Introducing Electrochemical Covalent Biolinkers

Chun Wang,[†,#] Nan Huang,[†,#] Hao Zhuang,[‡] and Xin Jiang*[,†,‡]

[†]Shenyang National Laboratory for Materials Science, Institute of Metal Research, Chinese Academy of Sciences, Wenhua Road 72, 110016 Shenyang, China

[‡]Institute of Materials Engineering, University of Siegen, Paul-Bonatz-Str. 9-11, 57076 Siegen, Germany

ABSTRACT: Zinc oxide (ZnO) is considered to be one of the most promising candidates for the third-generation DNA biosensor because of its good chemical stability, wonderful biocompatibility, easy surface modification, and numerous kinds of nanostructures. In this work, we report a new and simple method to modify ZnO surface for the immobilization of oligonucleotides by electrochemical covalent grafting of diazonium salts. The atomic force microscope, X-ray photoelectron spectroscopy, surface contact angle system, and electrochemical workstation were employed to characterize the functionalization process. Fluorescence results show that this kind of DNA biosensor from covalently linking strategy has an enhanced performance compared to that based on an electrostatic adsorption route. The functionalized ZnO biosensor has the capability to distinguish four-base mismatched, one-base mismatched, and complementary DNA sequences. Moreover, a linear relationship has been observed between the fluorescence intensity and the concentration of the complementary DNA in the solution within the range from 10^{-6} to 10^{-9} M, offering us a possibility in the qualitative determination of the level of target DNA.

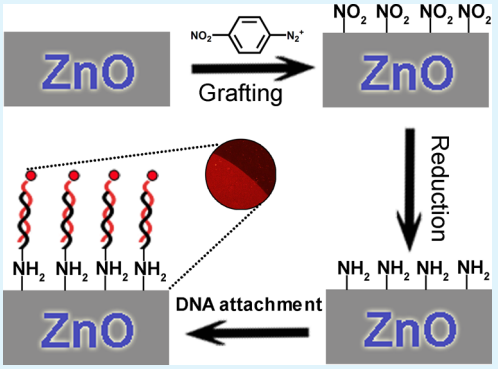

KEYWORDS: *ZnO, functionalization, covalent bond, electrochemistry, fluorescence, DNA biosensor*

INTRODUCTION

Many diseases such as tuberculosis,[1] sexually transmitted diseases,[2] and cancers are the result of some specific base sequences on DNA. Meanwhile, the mutation of DNA sequences has a strong relationship with specific diseases. Consequently, it is necessary to develop the DNA biosensor for the detection of specific DNA fragments. It is widely known that the solid platform for immobilizing probe DNA should be biocompatible, nontoxic, and chemically stable.[3] Gold, silicon, and carbon materials[4,5] were widely used as solid substrates to inspect the target DNA sequences. However, these DNA biosensors lack stability due to the gradual dissolution in aqueous solution, which in turn results in the degradation of the biosensing response.[5,6] Besides, the biocompatibility of silicon is reported to be quite limited.[7] Therefore, a new category of stable ceramic materials for linking the DNA molecule is urgently needed to improve the performance and the lifetime.

ZnO is a wide band gap (3.37 eV) material with novel mechanical and optical properties, high electron mobility, high exciton binding energy (60 meV), and low cost,[8] which is usually used in solar cells, short wavelength light emitters, acoustic wave devices, mechanical or piezoelectric sensors, and ultraviolet (UV) lasers.[9] Meanwhile, ZnO also has high chemical stability and good biocompatibility. It has a high isoelectric point (IPE) of ~9.5 and can be conductive by doping. Furthermore, the possible fabrication of various ZnO nanostructures such as nanowires, particles, flowers, and nanowalls with a large surface area also offer us more choices for specific applications.[10,11] Hence, ZnO is considered as one of the most promising candidates for the third generation of DNA biosensors.[12] Most of the reported ZnO biosensors are constructed by a principle of the weak physical and electrostatic adsorption.[13−15] However, such a weak bonding could cause the problem of the probe DNA biomolecule desorption during the sensing process, which leads to gradually deteriorated response. Furthermore, the hydrophobicity of bare ZnO surface also hinders the adsorption of biomolecules.[16] In contrast, ZnO biosensors have shown an enhanced performance, which are designed by the covalent biolinkers, such as thiol groups, carboxylic groups through fatty acid modification,[17] and amino groups via organosilane modification.[18,19] However, thiol and carboxylic bonding are strongly dependent on the structure of compounds as well as the experimental conditions. Moreover, acids may also etch ZnO, which limits their application.[17] Alternatively, amino groups can also be used to modify the electrode for biosensor applications.[20−22] Zhao et al. observed that, after amino groups functionalization via organosilanes, nonspecific adsorption of DNA onto the ZnO surface can be reduced.[18] Kumar et al. discovered that covalent amino groups

Received: January 5, 2015
Accepted: March 23, 2015
Published: March 23, 2015

DOI: 10.1021/acsami.5b00040
ACS Appl. Mater. Interfaces 2015, 7, 7605−7612

Scheme 1. Illustration of Fabricating ZnO Biosensors via Electrochemical Method

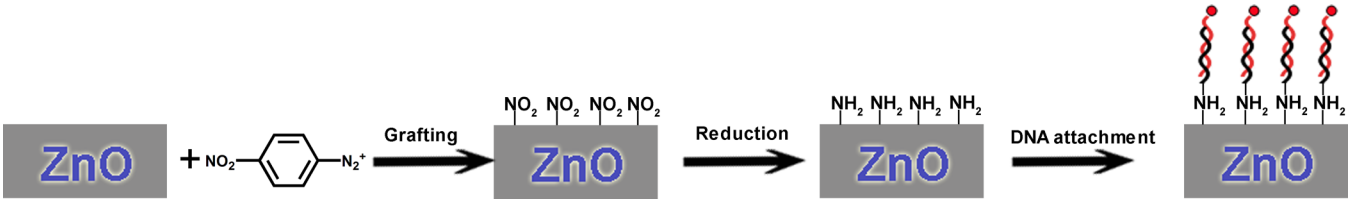

functionalization via organosilanes could improve the sensitivity of the ZnO-arrays-based biosensors.[19] However, covalent linking via organosilanes strongly depends on the concentration of hydroxyl groups.[23] In addition, to achieve a higher sensitivity, a monolayer of organosilane on the surface is preferred. This is, however, very difficult to achieve, which requires precise control of the trace amount of water on the ZnO surface.[24] In this context, developing a facile approach to link amino groups onto the ZnO surface becomes imperative. It was reported that amino groups can be introduced to the electrode surface by simple electrochemical attachment of diazonium salts with good controllability.[25] This functionalization strategy via the linkage of amino groups have been applied in metal surfaces,[26] carbon materials,[25,27] and silicon carbide[28] to improve the performance of biosensors. Compared with the above materials, ZnO is cheaper and easier to obtain and has been popularly used as a biosensor.[3] However, until date, the electrochemical grafting of diazonium salts to the ZnO surface has not yet been investigated. On the basis of the above discussion, in this work, the ZnO biosensor was designed for the first time by electrochemical grafting of amino groups using diazonium salts. Atomic force microscopy (AFM), X-ray photoelectron spectroscopy (XPS), and cyclic voltammetry results show the successful introduction of covalent biolinkers to the surface of ZnO. Decreased contact angle indicates that functionalized ZnO is more suitable for a biological system owing to the higher hydrophilicity. Finally, after the attachment of target DNA molecule, the performances of this kind of ZnO biosensor were characterized by an electrochemical workstation and fluorescence microscope compared with that based on physical adsorption.

EXPERIMENTAL SECTION

Materials and Instruments. Nanocrystalline aluminum (Al)-doped ZnO films were purchased from Kaiwo China, which were fabricated by a sputtering method on the glass substrates. 4-Nitrobenzenediazonium tetrafluoroborate, tetrabutylammonium tetrafluoroborate ($TBABF_4$), and sulfosuccinimidyl-4-(*N*-maleimidomethyl) cyclohexane-1-carboxylate (SSMCC) were purchased from Sigma-Aldrich. All chemical reagents were of analytical grade and used as received without further purification. Aqueous solutions were prepared with deionized water (18.2 MΩ·cm) produced by a Millipore Milli-Q system.

DNA used for detection was bought from TaKaRa, and the sequences are as follows: 5′-HS-C_6H_{12}-T_6-GCTTATC-GAGCTTTCG-3′ (probe sequences); 5′Cy5-CGAAAGCTC-GATAAGC-3′ (complementary sequences); 5′-Cy5-CGAA*T*GCTCGATAAGC-3′ (one-base mismatched sequences); 5′-Cy5-CGA*TT*GCTC*CT*TAAGC-3′ (four-base mismatched sequences), where Cy5 indicates a red fluorescence marker. As the target DNA is labeled with Cy5 fluorescence label, after hybridization, a fluorescence signal can be observed. The fluorescence intensity can be used to detect the amount of target DNA. According to the intensity of the fluorescence signal, it would be possible to quantitatively determine the amount of DNA on the ZnO surface.

The crystal structure of ZnO films were examined by a Rigaku RINT 2000 X-ray powder diffractometer (XRD) with Cu Kα radiation, and the scanning electron microscope (SEM) images were recorded on Zeiss Supra 55. AFM surface morphologies were examined on an Innova system from Bruker. For XPS measurements, a monochromated Al Kα beam was used as an X-ray source. The contact angles of samples were examined by a Dataphysics 15EC contact angle analyzer. The fluorescence images were recorded on an Olympus BX51 microscope. An Autolab PGSTAT302N workstation was used for electrochemical experiments. A conventional three-electrode system was employed with a ZnO film as a working electrode and a platinum wire as a counter electrode. A Ag/Ag^+ (0.01 M) reference electrode was used in organic solvents while a Ag/AgCl (3 M KCl) reference electrode was applied in aqueous solutions.

Methods. The fabrication of ZnO biosensors is shown in Scheme 1. The grafting of ZnO films was performed in dehydrated acetonitrile containing 1.0 mM 4-nitrobenzene diazonium salts with 0.1 M $TBABF_4$ as supporting electrolyte. For cyclic voltammetry, the initial, upper, and lower potentials were 0, 0.2, and −0.8 V (vs Ag/Ag^+) and the scanning rate was 200 mV s^{-1}. After grafting, the electrochemical behavior of the modified ZnO was recorded in blank solution (dehydrated acetonitrile containing 0.1 M $TBABF_4$). And the surface was reduced in 0.1 M KCl solution of $C_2H_5OH-H_2O$ (V/V = 1:9) solvent for the next DNA attachment step, the scanning range was between 0.5 and −1.5 V (vs Ag/AgCl), and the scanning rate was 100 mV s^{-1}.

After the reduction process, the modified ZnO surface was soaked in 1.5 mM solution of the SSMCC as cross-linker for 20 min at room temperature; 2 μL probe DNA oligonucleotides were then put on the modified surface with SSMCC cross-linked at 37 °C in the humid box while the other 2 μL target DNA were placed on the sensor surface overnight. After each step, the sample surface was washed with deionized water to remove adsorbed molecules. To study the different performances of the ZnO DNA biosensor covalently linked and physically absorbed, respectively, the center area of ZnO film was modified by electrochemical grafting and cross-linker introduction. Then the whole ZnO surface except the margin was exposed to probe DNA. After incubation, the covalent/physical adsorption ZnO DNA biosensor was used to detect the target DNA. To investigate sensitivity of the biosensor, the concentration of target DNA was varied from 10^{-6} to 10^{-9} M. Three different DNA sequences were used to reveal the selectivity of the biosensor.

DOI: 10.1021/acsami.5b00040
ACS Appl. Mater. Interfaces 2015, 7, 7605−7612

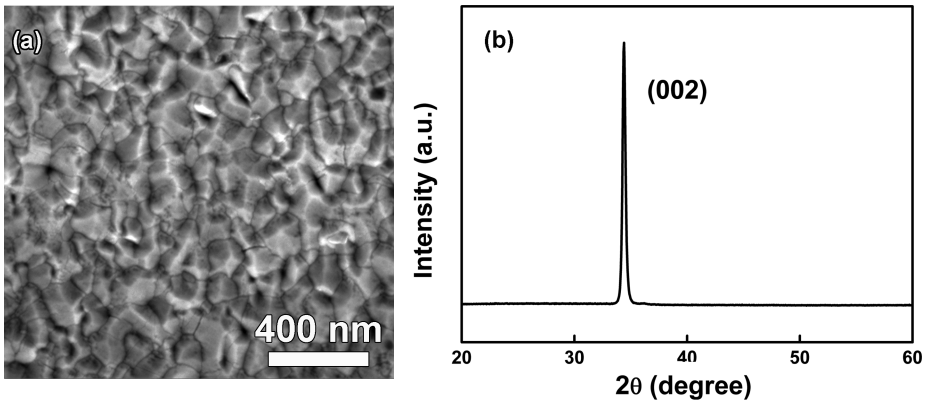

Figure 1. High-resolution SEM image (a) and XRD spectrum (b) of a ZnO film.

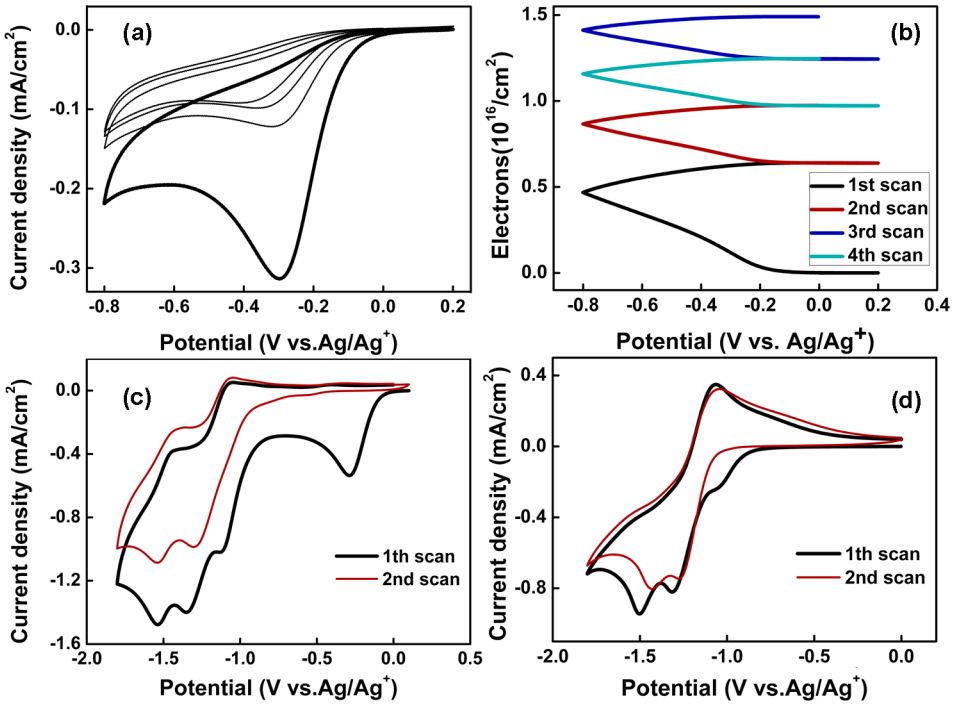

Figure 2. Cyclic voltammograms of electrochemical grafting nitrophenyl layers onto ZnO in 0.1 M $TBABF_4$ solution containing 1 mM 4-nitrobenzene diazonium salts: (a) scanning range, from 0.2 to −0.8 V (vs Ag/Ag^+); (b) density of transferring electrons during (a); (c) larger scanning range, from 0 to −1.8 V (vs Ag/Ag^+); and (d) cyclic voltammograms in 0.1 M $TBABF_4$ solution (blank solution) after (a) and scanning range from 0.2 to −0.8 V (vs Ag/Ag^+).

RESULTS AND DISCUSSION

Figure 1a shows the surface morphology of the ZnO film prepared on the glass substrates by a magnetron sputtering method. The grain size is about 50−200 nm. The sheet resistivity is measured to be 9.3 ± 0.1 Ω/sq. by the four-point probe method. The XRD spectrum of the film shows a typical wurtzite structure of ZnO in Figure 1b. The presence of only the diffraction peak corresponding to the (002) reflex indicates the preferential orientation of ZnO with the *c*-axis perpendicular to the substrate surface.

Cyclic voltammograms of electrochemical grafting of 4-nitrophenyl ($C_6H_5-NO_2$) groups onto the surface of ZnO electrode are shown in Figure 2a. The first cycle (the thicker line) shows an irreversible reduction peak centered at about −0.27 V (vs Ag/Ag^+). This is due to the reduction of diazonium salts which generates active aryl radicals ($\cdot C_6H_5-NO_2$) covalently bonding to ZnO surface.[29,30] It was noticed that the peak current decreases significantly during the second scan and shifts to more negative potential in subsequent cycles (the thinner lines). Such a phenomenon can be attributed to the formation of insulating $C_6H_5-NO_2$ layers on ZnO during the grafting process,[31] which in turn blocks further electron transfer. This can also be reflected by the continuous decrease of current during the positive scan. The current after the turning point is negative and stays negative even at positive potential; this characteristic shape of the reverse scan curve also reveals the occurrence of self-inhibition.[32] Forty-three percent of the total electron density of 1.5×10^{16} cm^{-2} is exchanged during the first cycle (Figure 2b) while the number of exchanged electrons decreases with increasing cycles.

Nevertheless, the cathodic peak is still observable even after four cycles. This behavior is similar to that of the SiC electrode,[33] but different from that on the diamond surface. For the case of the diamond electrode, this peak quickly disappears

DOI: 10.1021/acsami.5b00040
ACS Appl. Mater. Interfaces 2015, 7, 7605−7612

after only one cycle,[34] indicating the forming of $C_6H_5-NO_2$ layers on the diamond surface is much faster than that on ZnO films. The reason might be that a greater proportion of radicals produced by reduction of the diazonium salts diffuse and react in the solution rather than attach to the ZnO electrode surface.[27] When the electrochemical scanning range of grafting is larger, other waves appear (Figure 2c). An irreversible cathodic peak (−1.12 V vs Ag/Ag^+) appears in the first scan which is probably caused by a small amount of unattached diazonium salts and disappears in the second scan. While the other two reversible cathodic peaks (−1.32 and −1.50 V vs Ag/Ag^+) still exist in the second cycle and their positions turn to more positive potential. The decreasing peaks during the second scan indicate the forming of insulating $C_6H_5-NO_2$ films. Those two peaks are related to the two-electron reduction process of the NO_2 group in the $C_6H_5-NO_2$ layers.[25] Such a phenomenon is similar to that of diamond, but different from one-electron redox reaction on glassy carbon and other carbon materials,[31,35] which implies the dianion species are more stable on ZnO and ZnO electrode can enhance voltammetric resolution.[34]

After electrochemical grafting of $C_6H_5-NO_2$ groups onto ZnO electrode, the electrochemical response of $C_6H_5-NO_2$ layers on ZnO in 0.1 M $TBABF_4$ solution (blank solution) is shown in Figure 2d. There is only one anodic peak while three cathodic peaks appear during the first scan. The first cathodic peak (−1.03 V vs Ag/Ag^+) is similar to that of diazonium salts grafting as shown in Figure 2c and disappears in the second scan, which is perhaps caused by a small amount of adsorbed diazonium salts. The other two cathodic peaks are related to the two-electron reduction of NO_2 group in the $C_6H_5-NO_2$ layers.[25] The anodic peak (−1.06 V vs Ag/Ag^+) is only due to the one-electron oxidation of $C_6H_5-NO_2$ molecules attached to ZnO surface. However, its shape is not similar to its corresponding cathodic peak. The reason is that the cathodic wave is also influenced by the decomposition of supporting electrolyte and the reduction of trace impurities.[35] The absence of dianion anodic peak indicates dianion species are not stable enough in blank solution, and further study is necessary. The roughnesses (Rq) of ZnO surface before and after grafting of 4-nitrophenyl groups were measured by AFM measurement. As shown in Figure 3a, the roughness of bare ZnO is 11.9 nm. After grafting, the roughness of surfaces is 21.8 nm (Figure 3b) and it indicates the modified ZnO surface is rougher than the bare one.

4-Nitrophenyl-modified ZnO also can be reduced in the solution of 0.1 M KCl in $C_2H_5OH-H_2O$ (V/V = 1:9) solvent (Figure 4). During the first scan, an irreversible reduction peak appears at −0.86 V (vs Ag/AgCl). This cathodic wave is

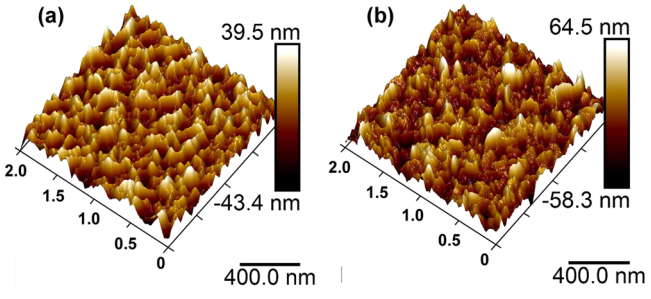

Figure 3. AFM surface images of (a) a bare ZnO film and (b) 4-nitrophenyl layer on ZnO.

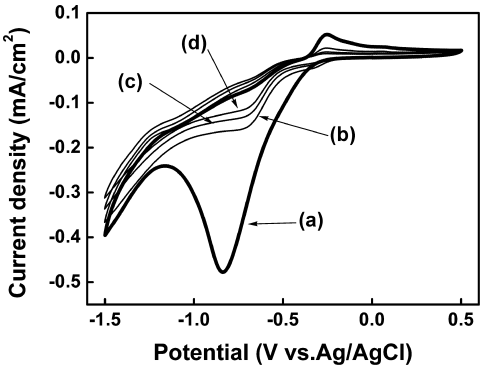

Figure 4. Cyclic voltammograms of reduction of nitrophenyl films on ZnO in solution ($C_2H_5OH-H_2O$ (V/V = 1:9)) containing 0.1 M KCl; scanning rate, 100 mV s^{-1}. (a) First scan; (b)−(d) second to fourth scans.

induced by an overall 6 e^- two-step electrochemical reduction of 4-nitrophenyl to aminophenyl ($C_6H_5-NH_2$).[36] During the process, hydroxyaminophenyl (C_6H_5-NHOH) is formed as intermediate product.[37] In the subsequent cycles, this reduction peak drastically diminishes, indicating that most of $C_6H_5-NO_2$ groups are reduced in the first scan. During the anodic scan, reversible redox peaks appear at $E_{1/2}$ = −0.28 V (vs Ag/AgCl), which results from the hydroxyaminophenyl/nitrosophenyl interconversion.[28,37] As a result, the reduction process of $C_6H_5-NO_2$ into $C_6H_5-NH_2$ during the cathodic scan is incomplete. The currents of the oxidation/reduction peaks will decrease with the increasing scans and finally disappear after enough rounds of scanning. This is caused by the coupling reaction of $C_6H_5-NO_2$ groups with $C_6H_5-NH_2$ groups to generate either azo or azoxy compounds, which inactivates the grafted film.[38] In this work, there are a few coupling reactions for only four cycles of scanning and still enough $C_6H_5-NH_2$ groups for the next DNA attachment step.

The surface modification can be further confirmed by the XPS measurement. As shown in Figure 5, the N(1s) is not

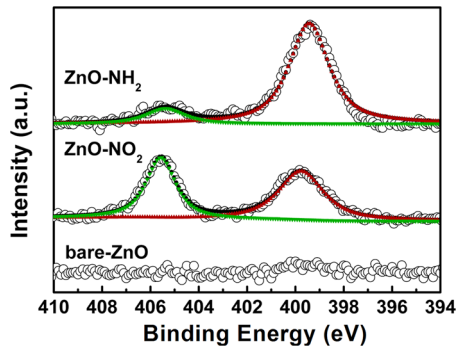

Figure 5. N(1s) XPS spectra (405.9 eV, NO_2 group; 399.8 eV, reduced groups) of a bare ZnO film, 4-nitrophenyl layers on ZnO(ZnO−NO_2), and after reduction of 4-nitrophenyl groups on ZnO(ZnO−NH_2).

observable on the bare ZnO. After grafting of $C_6H_5-NO_2$ groups to ZnO surface, two peaks emerge. The peak located at 405.9 eV corresponds to NO_2 group, which indicates the successful grafting of the diazonium salts. A minor peak locating at 399.8 eV is also observable, which is due to the reduction of the NO_2 groups into NH_2 groups.[38] After the reduction of $C_6H_5-NO_2$ groups, the peak at 406 eV decreases while the

DOI: 10.1021/acsami.5b00040
ACS Appl. Mater. Interfaces 2015, 7, 7605−7612

peak at 399.8 eV increases, implying that a significant amount of $C_6H_5-NO_2$ groups has been reduced to $C_6H_5-NH_2$ groups.[26] Nevertheless, the existence of the N(1s) (405.9 eV) peak indicates the conversion is incomplete, which is in good accordance with the cyclic voltammetry results shown in Figure 4.

Surface wettability is an important factor for considering the application of electrodes in biological systems. This is because specific biomolecule adsorption will be promoted or suppressed by tuning the surface hydrophobicity/hydrophilicity.[35,39] In accordance with previous reports,[40] the water contact angle of the bare ZnO is 104.0 ± 3.3°, indicating the bare ZnO is hydrophobic. Such a hydrophobic surface might hinder the approaching of biomolecules in the solution to the surface, which reduces the amount of immobilized biomolecules on the surface.[16] After grafting of $C_6H_5-NO_2$, the water contact angle decreases to about 90° due to the large amount of NO_2 group. However, the surface is still hydrophobic to a certain extent as shown in Figure 6. After reduction, a greater portion of groups

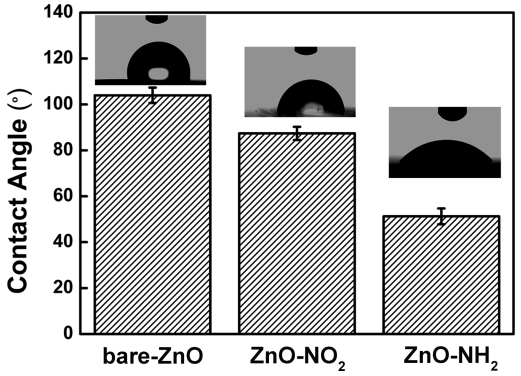

Figure 6. Contact angles of a bare ZnO film, 4-nitrophenyl layers coated ZnO(ZnO−NO_2), and after the reduction of 4-nitrophenyl groups on ZnO(ZnO−NH_2).

such as $C_6H_5-NH_2$ and C_6H_5NHOH groups form, rendering a hydrophilic surface with a water contact angle of 51.2 ± 3.5°. The result is similar to that of the modified ultra-nanocrystalline diamond (contact angle =55.3 ± 2.9°).[35] The above results not only show the versatility of electrochemical functionalization of ZnO using diazonium salts but also imply the superiority of ZnO as the electrode for electrochemistry in organic solution. The improved hydrophilicity of the functionalized ZnO could be beneficial for the detection of biomolecules in aqueous biological systems.[16,41]

After modification, the electrochemical behavior of ZnO electrode may be different since the insulating organic films might hold back the transfer of electrons and restrict the performance of ZnO biosensor. To clarify this, $Fe(CN)_6^{3-/4-}$ (inner-sphere transfer mechanism) and $Ru(NH_3)_6^{2+/3+}$ (outer-sphere transfer mechanism) were used to measure the change of electrochemical behavior of the ZnO electrode before and after functionalization. As shown in Figure 7a, symmetric redox peaks of $Fe(CN)_6^{3-/4-}$ are recorded on bare ZnO at $E_{1/2}$ = 0.23 V (vs Ag/AgCl). Its electrical response is totally suppressed on the $C_6H_5-NO_2$ modified surface, which is due to the presence of $C_6H_5-NO_2$ groups as a physical barrier.[38] After reduction, a large quantity of NHOH and NH_2 groups enhance the electron transfer and the defects generated during the reduction process also allow $Fe(CN)_6^{3-/4-}$ species to reach the ZnO surface. As a result, the overall response of $Fe(CN)_6^{3-/4-}$ is similar to that on the bare ZnO electrode. In contrast to the $Fe(CN)_6^{3-/4-}$ system, the response of $Ru(NH_3)_6^{2+/3+}$ (Figure 7b) is less affected by the transformation of the electrode surface condition; symmetric redox peaks of $Ru(NH_3)_6^{2+/3+}$ are recorded on the bare ZnO at $E_{1/2}$ = 0.16 V (vs Ag/AgCl). Their intensities decrease slightly after $C_6H_5-NO_2$ functionalization. After reduction, a small shoulder appears along with the redox peaks. This is probably due to the slight stripping of organic layers on ZnO, which is noncovalently attached to the surface. According to the literature, it could be suppressed in the solution with the lower pH value due to the protonation of NH_2 groups.[38] On the basis of the above results, the electrochemical response of functionalized ZnO is not deteriorated and still suitable for electrochemical analysis. Therefore, ZnO platform via electrochemical immobilization of DNA molecules shows a great potential for an electrochemical biosensor. Such work is beyond the main scope of the present study and is underway in our lab.

After functionalization, probe DNA (ss-DNA) was further linked to the functionalized ZnO and hybridized with its complementary DNA (cy5, a red fluorescence label at the 5′ end to detect DNA target molecules) to form double-stranded DNA (ds-DNA). The hybridization process is monitored using a fluorescence microscope. As shown in Figure 8, three different regions with different fluorescence intensities can be observed. Region 1 shows the bare ZnO area without any probe DNA molecule. Region 2 represents the ZnO with only physically

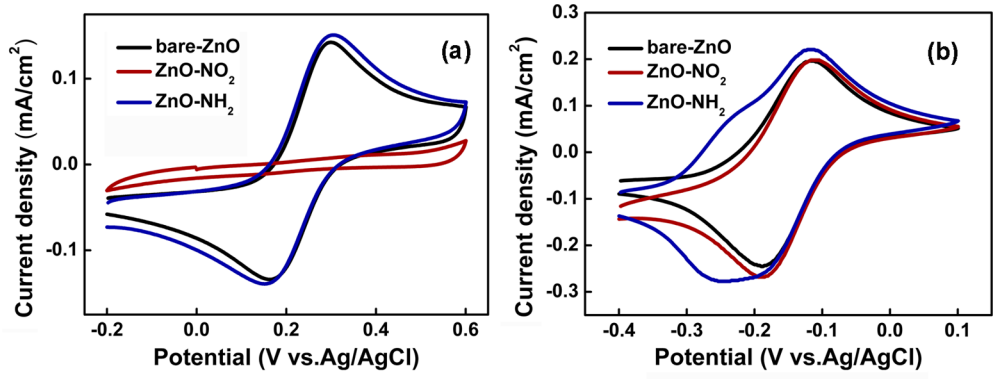

Figure 7. Cyclic voltammograms in 1 mM $Fe(CN)_6^{3-/4-}$ (a) and 1 mM $Ru(NH_3)_6^{2+/3+}$ (b) solution of bare ZnO film, 4-nitrophenyl layers on ZnO(ZnO−NO_2), and after reduction of 4-nitrophenyl groups on ZnO(ZnO−NH_2).

DOI: 10.1021/acsami.5b00040
ACS Appl. Mater. Interfaces 2015, 7, 7605−7612

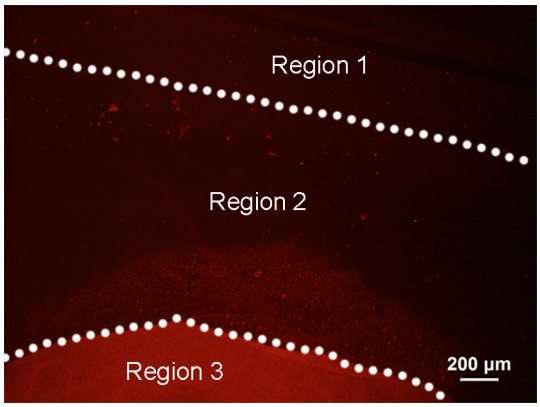

Figure 8. Fluorescence image of bare ZnO (region 1) and ds-DNA-functionalized ZnO without (region 2) or with (region 3) biolinkers.

adsorbed ss-DNA. Region 3 depicts the functionalized ZnO with covalently attached ss-DNA. Clear differences can be observed. For the case of region 3, where ZnO is functionalized with diazonium salts, strong fluorescence signal from the Cy5 label can be observed. This indicates that the ss-DNA has been linked to the surface of ZnO film via the amino groups and is still bioactive. The fluorescence signals of bare ZnO film and physically adsorbed region show no obvious difference and the intensity is weak. Such a phenomenon indicates that no detectable physical adsorption of DNA presents in the present study, which is beneficial in obtaining a high signal-to-noise ratio during fabricating ZnO-based DNA biosensor.

While talking about DNA biosensors, it is essential to distinguish DNA with only a slight difference in their sequences, i.e., one-base mismatched DNA. This is because a small disparity in genetic code can result in the significant variations in phenotypes and biologically activated micro-organisms.[19] To clarify this point, the detection of one-base mismatched DNA, four-base mismatched DNA, and complementary DNA was carried out on the functionalized ZnO surface. As shown in Figure 9a, the fluorescence results illustrate almost no difference between four-base mismatched sequences functionalized area and bare ZnO, which indicates no hybridization occurs on the surface. When one-base mismatched DNA is employed, a relatively weak fluorescence signal is observed, indicating the occurrence of a slight hybridization. This is expected that ss-DNA and one-base mismatched DNA can form ds-DNA during the molecular recognition process, but this duplex is weaker than that formed by ss-DNA and its complementary DNA.[42] Nevertheless, its intensity is only about 30% of that of complementary sequences. According to the above results, the ZnO biosensor has very good selectivity for DNA sequences detection. Besides, it is also possible to distinguish the amount of complementary DNA in the solution by measuring the intensity of the fluorescence signal. As shown in Figure 9b, the fluorescence signal increases linearly with the logarithm of the concentration of the target DNA in the solution in the concentration range from 10^{-6} to 10^{-9} M. This offers us a possibility in the qualitative determination of the concentration of target DNA in the solution. Moreover, lifetime is an important concern during the fabrication of DNA biosensor, and in our future work, we will seriously take the lifetime into consideration. Meanwhile, we are making the electrochemical detection of DNA in the real sample. And then, the ZnO biosensor was used to detect the complementary DNA several times. The intensities of fluorescence signals for the same concentration of target DNA change slightly, showing the biosensor has good reproducibility.

CONCLUSIONS

In summary, diazonium salts were reduced electrochemically to $C_6H_5-NH_2$ groups and used to functionalize ZnO surface. Successful functionalization is confirmed by electrochemical response, AFM, XPS results, and contact angle measurements. Probe DNA was covalently electrochemically bonded to the surface of ZnO via the $C_6H_5-NH_2$ groups for the detection of the target DNA in the solution in a fluorescence microscope. The functionalized ZnO surface shows good sensitivity and selectivity for the target DNA, which is able to distinguish four-base mismatched, one-base mismatched, and complementary DNA. Moreover, a linear relationship within the range from 10^{-6} to 10^{-9} M has been observed between the fluorescence signal and the logarithm of the concentration of the target DNA in the solution.

AUTHOR INFORMATION

Corresponding Author

*E-mail: xjiang@imr.ac.cn.

Author Contributions

#These authors contributed equally to this work.

Notes

The authors declare no competing financial interest.

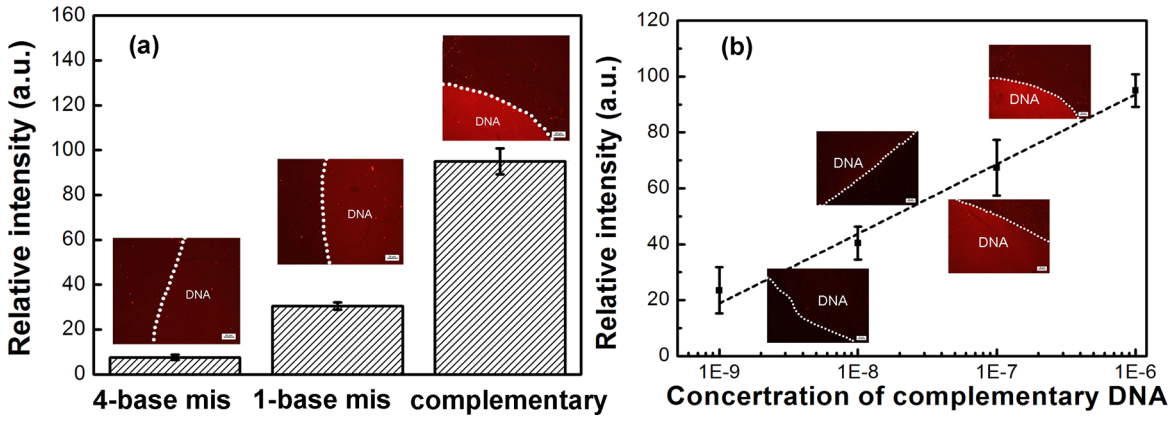

Figure 9. Fluorescence images of different sequences (a) and concentration (b) of ds-DNA-functionalized ZnO.

DOI: 10.1021/acsami.5b00040
ACS Appl. Mater. Interfaces 2015, 7, 7605−7612

■ ACKNOWLEDGMENTS

We sincerely acknowledge financial support from the Project supported by the National Natural Science Foundation of China (Grant No. 51202257) and Liaoning Province Doctoral Scientific Research Foundation of China (Grant No. 20131121). We also thank Dr. Nianjun Yang in Siegen University for valuable discussion and suggestions.

■ REFERENCES

(1) Das, M.; Sumana, G.; Nagarajan, R.; Malhotra, B. D. Application of Nanostructured ZnO Films for Electrochemical DNA Biosensor. *Thin Solid Films* **2010**, *519*, 1196−1201.
(2) Ansari, A. A.; Singh, R.; Sumana, G.; Malhotra, B. D. Sol-Gel Derived Nano-Structured Zinc Oxide Film for Sexually Transmitted Disease Sensor. *Analyst* **2009**, *134*, 997−1002.
(3) Arya, S. K.; Saha, S.; Ramirez-Vick, J. E.; Gupta, V.; Bhansali, S.; Singh, S. P. Recent Advances in ZnO Nanostructures and Thin Films for Biosensor Applications: Review. *Anal. Chim. Acta* **2012**, *737*, 1−21.
(4) Herne, T. M.; Tarlov, M. J. Characterization of DNA Probes Immobilized on Gold Surfaces. *J. Am. Chem. Soc.* **1997**, *119*, 8916−8920.
(5) Strother, T.; Cai, W.; Zhao, X. S.; Hamers, R. J.; Smith, L. M. Synthesis and Characterization of DNA-Modified Silicon (111) Surfaces. *J. Am. Chem. Soc.* **2000**, *122*, 1205−1209.
(6) Yang, W. S.; Auciello, O.; Butler, J. E.; Cai, W.; Carlisle, J. A.; Gerbi, J.; Gruen, D. M.; Knickerbocker, T.; Lasseter, T. L.; Russell, J. N.; Smith, L. M.; Hamers, R. J. DNA-Modified Nanocrystalline Diamond Thin-Films as Stable, Biologically Active Substrates. *Nat. Mater.* **2002**, *1*, 253−257.
(7) Stutzmann, M.; Garrido, J. A.; Eickhoff, M.; Brandt, M. S. Direct Biofunctionalization of Semiconductors: A Survey. *Phys. Status Solidi A* **2006**, *203*, 3424−3437.
(8) Huang, N.; Sun, C.; Zhu, M. W.; Zhang, B.; Gong, J.; Jiang, X. Microstructure Evolution of Zinc Oxide Films Derived from Dip-Coating Sol-Gel Technique: Formation of Nanorods through Orientation Attachment. *Nanotechnology* **2011**, *22*, 1−9.
(9) Wang, Z. L. Zinc Oxide Nanostructures: Growth, Properties and Applications. *J. Phys.: Condens. Matter* **2004**, *16*, R829−R858.
(10) Israr, M. Q.; Sadaf, J. R.; Nur, O.; Willander, M.; Salman, S.; Danielsson, B. Chemically Fashioned ZnO Nanowalls and Their Potential Application for Potentiometric Cholesterol Biosensor. *Appl. Phys. Lett.* **2011**, *98*, 253705-1−253701-3.
(11) Pradhan, D.; Niroui, F.; Leung, K. T. High-Performance, Flexible Enzymatic Glucose Biosensor Based on ZnO Nanowires Supported on a Gold-Coated Polyester Substrate. *ACS Appl. Mater. Interfaces* **2010**, *2*, 2409−2412.
(12) Gupta, V. ZnO Based Third Generation Biosensor. *Thin Solid Films* **2010**, *519*, 1141−1144.
(13) Zhang, F. F.; Wang, X. L.; Ai, S. Y.; Sun, Z. D.; Wan, Q.; Zhu, Z. Q.; Xian, Y. Z.; Jin, L. T.; Yamamoto, K. Immobilization of Uricase on ZnO Nanorods for a Reagentless Uric Acid Biosensor. *Anal. Chim. Acta* **2004**, *519*, 155−160.
(14) Solanki, P. R.; Kaushik, A.; Ansari, A. A.; Malhotra, B. D. Nanostructured Zinc Oxide Platform for Cholesterol Sensor. *Appl. Phys. Lett.* **2009**, *94*, 143901-1−143901-3.
(15) You, X.; Pikul, J. H.; King, W. P.; Pak, J. J. Zinc Oxide Inverse Opal Enzymatic Biosensor. *Appl. Phys. Lett.* **2013**, *102*, 253103-1−253013-4.
(16) Wu, S.; Wu, H.; Liu, Y. Y.; Ju, H. X. Conductive and Highly Catalytic Nanocage for Assembly and Improving Function of Enzyme. *Chem. Mater.* **2008**, *20*, 1397−1403.
(17) Taratula, O.; Galoppini, E.; Wang, D.; Chu, D.; Zhang, Z.; Chen, H. H.; Saraf, G.; Lu, Y. C. Binding Studies of Molecular Linkers to ZnO and MgZnO Nanotip Films. *J. Phys. Chem. B* **2006**, *110*, 6506−6515.
(18) Zhao, J.; Wu, L.; Zhi, J. Fabrication of Micropatterned ZnO/SiO_2 Core/Shell Nanorod Arrays on a Nanocrystalline Diamond Film and Their Application to DNA Hybridization Detection. *J. Mater. Chem.* **2008**, *18*, 2459−2465.
(19) Kumar, N.; Dorfman, A.; Hahm, J. Ultrasensitive DNA Sequence Detection Using Nanoscale ZnO Sensor Arrays. *Nanotechnology* **2006**, *17*, 2875−2881.
(20) Zhuang, H.; Srikanth, V. V. S. S.; Jiang, X.; Aronov, I.; Wenclawiak, B. W.; Luo, J.; Ihmels, H. Elucidation of Different Steps Involved in Allylamine Functionalization of the Diamond Surface and Its Polymerization by Time-of-Flight Secondary Ion Mass Spectrometry. *Chem. Mater.* **2010**, *22*, 4414−4418.
(21) Zhuang, H.; Srikanth, V. V. S. S.; Jiang, X.; Luo, J.; Ihmels, H.; Aronov, I.; Wenclawiak, B. W.; Adlung, M.; Wickleder, C. Allylamine-Mediated DNA Attachment to Polycrystalline Diamond Surface. *Appl. Phys. Lett.* **2009**, *95*, 143703-1−143703-3.
(22) Zhuang, H.; Jiang, X. In *PRICM 8: The Eighth Pacific Rim International Congress on Advanced Materials and Processing*; Marquis, F., Ed.; John Wiley & Sons, Inc.: Hoboken, NJ, 2013; pp 1853−1861.
(23) Kim, H.; Colavita, P. E.; Paoprasert, P.; Gopalan, P.; Kuech, T. F.; Hamers, R. J. Grafting of Molecular Layers to Oxidized Gallium Nitride Surfaces via Phosphonic Acid Linkages. *Surf. Sci.* **2008**, *602*, 2382−2388.
(24) Dkhissi, A.; Esteve, A.; Jeloaica, L.; Esteve, D.; Rouhani, M. D. Self-Assembled Monolayers and Preorganization of Organosilanes Prior to Surface Grafting onto Silica: A Quantum Mechanical Study. *J. Am. Chem. Soc.* **2005**, *127*, 9776−9780.
(25) Uetsuka, H.; Shin, D.; Tokuda, N.; Saeki, K.; Nebel, C. E. Electrochemical Grafting of Boron-Doped Single-Crystalline Chemical Vapor Deposition Diamond with Nitrophenyl Molecules. *Langmuir* **2007**, *23*, 3466−3472.
(26) Bernard, M. C.; Chausse, A.; Cabet-Deliry, E.; Chehimi, M. M.; Pinson, J.; Podvorica, F.; Vautrin-Ul, C. Organic Layers Bonded to Industrial, Coinage, and Noble Metals through Electrochemical Reduction of Aryldiazonium Salts. *Chem. Mater.* **2003**, *15*, 3450−3462.
(27) Allongue, P.; Delamar, M.; Desbat, B.; Fagebaume, O.; Hitmi, R.; Pinson, J.; Saveant, J. M. Covalent Modification of Carbon Surfaces by Aryl Radicals Generated from the Electrochemical Reduction of Diazonium Salts. *J. Am. Chem. Soc.* **1997**, *119*, 201−207.
(28) Yang, N. J.; Zhuang, H.; Hoffmann, R.; Smirnov, W.; Hees, J.; Jiang, X.; Nebel, C. E. Nanocrystalline 3C-SiC Electrode for Biosensing Applications. *Anal. Chem.* **2011**, *83*, 5827−5830.
(29) Yang, N. J.; Uetsuka, H.; Nebel, C. E. Biofunctionalization of Vertically Aligned Diamond Nanowires. *Adv. Funct. Mater.* **2009**, *19*, 887−893.
(30) Saby, C.; Ortiz, B.; Champagne, G. Y.; Belanger, D. Electrochemical Modification of Glassy Carbon Electrode Using Aromatic Diazonium Salts 0.1. Blocking Effect of 4-Nitrophenyl and 4-Carboxyphenyl Groups. *Langmuir* **1997**, *13*, 6805−6813.
(31) Delamar, M.; Hitmi, R.; Pinson, J.; Saveant, J. M. Covalent Modification of Carbon Surfaces by Grafting of Functionalized Aryl Radicals Produced from Electrochemical Reduction of Diazonium Salts. *J. Am. Chem. Soc.* **1992**, *114*, 5883−5884.
(32) Bhugun, I.; Saveant, J. M. Derivatization of Surfaces and Self-Inhibition in Irreversible Electrochemical Reactions - Cyclic Voltammetry and Preparative-Scale Electrolysis. *J. Electroanal. Chem.* **1995**, *395*, 127−131.
(33) Yang, N. J.; Zhuang, H.; Hoffmann, R.; Smirnov, W.; Hees, J.; Jiang, X.; Nebel, C. E. Electrochemistry of Nanocrystalline 3C Silicon Carbide Films. *Chem. - Eur. J.* **2012**, *18*, 6514−6519.
(34) Shin, D. C.; Tokuda, N.; Rezek, B.; Nebel, C. E. Periodically Arranged Benzene-Linker Molecules on Boron-Doped Single-Crystalline Diamond Films for DNA Sensing. *Electrochem. Commun.* **2006**, *8*, 844−850.
(35) Jian, W.; Firestone, M. A.; Auciello, O.; Carlisle, J. A. Surface Functionalization of Ultrananocrystalline Diamond Films by Electrochemical Reduction of Aryldiazonium Salts. *Langmuir* **2004**, *20*, 11450−11456.
(36) Tsutsumi, H.; Furumoto, S.; Morita, M.; Matsuda, Y. Electrochemical-Behavior of a 4-Nitrothiophenol Modified Electrode

DOI: 10.1021/acsami.5b00040
ACS Appl. Mater. Interfaces 2015, 7, 7605−7612

Prepared by the Self-Assembly Method. *J. Colloid Interface Sci.* **1995**, *171*, 505−511.
(37) Brooksby, P. A.; Downard, A. J. Electrochemical and Atomic Force Microscopy Study of Carbon Surface Modification via Diazonium Reduction in Aqueous and Acetonitrile Solutions. *Langmuir* **2004**, *20*, 5038−5045.
(38) Ortiz, B.; Saby, C.; Champagne, G. Y.; Belanger, D. Electrochemical Modification of a Carbon Electrode Using Aromatic Diazonium Salts. 2. Electrochemistry of 4-Nitrophenyl Modified Glassy Carbon Electrodes in Aqueous Media. *J. Electroanal. Chem.* **1998**, *455*, 75−81.
(39) Zhuang, H.; Song, B.; Srikanth, V. V. S. S.; Jiang, X.; Schonherr, H. Controlled Wettability of Diamond/Beta-SiC Composite Thin Films for Biosensoric Applications. *J. Phys. Chem. C* **2010**, *114*, 20207−20212.
(40) Huang, L.; Lau, S. P.; Yang, H. Y.; Leong, E. S. P.; Yu, S. F.; Prawer, S. Stable Superhydrophobic Surface via Carbon Nanotubes Coated with a ZnO Thin Film. *J. Phys. Chem. B* **2005**, *109*, 7746−7748.
(41) Liu, M. C.; Zhao, G. H.; Zhao, K. J.; Tong, X. L.; Tang, Y. T. Direct Electrochemistry of Hemoglobin at Vertically-Aligned Self-Doping TiO_2 Nanotubes: A Mediator-Free and Biomolecule-Substantive Electrochemical Interface. *Electrochem. Commun.* **2009**, *11*, 1397−1400.
(42) Tawa, K.; Knoll, W. Mismatching Base-Pair Dependence of the Kinetics of DNA-DNA Hybridization Studied by Surface Plasmon Fluorescence Spectroscopy. *Nucleic Acids Res.* **2004**, *32*, 2372−2377.

DOI: 10.1021/acsami.5b00040
ACS Appl. Mater. Interfaces 2015, 7, 7605−7612